

Efficient parallel imaging strategies for Time-of-Flight venography with continuously moving table

M. Honal¹, and S. Huff¹

¹Dept. of Diagnostic Radiology, Medical Physics, University Hospital Freiburg, Freiburg, Germany

Introduction

Subtraction Time-of-flight (TOF) venography has recently been introduced as a method to image the veins of the entire legs with continuously moving table [1]. The acquisition time is an important issue for that method. In this study two variants of the GRAPPA algorithm [2] are investigated which avoid the acquisition of extra k-space lines for calibration. The z-GRAPPA algorithm [3] combines calibration data from spatially adjacent slices. The second method denoted as c-GRAPPA explicitly takes the subtraction TOF venography acquisition scheme into account. This technique is based on the subtraction of two images per slice position where the blood signal of the arteries only or the arteries and the veins are saturated respectively. Compared to conventional GRAPPA no significant loss of image quality could be observed for the experiments conducted for this study.

Methods

For the subtraction TOF venography two data sets are acquired. In the first acquisition, referred to as AVSat, the signal from the arterial and the venous inflow is saturated which yields an image volume where the signal of all blood vessels is suppressed. In the second acquisition, referred to as ASat, only the signal from the arterial inflow is saturated such that only the venous signal is present in the resulting image volume. Subtraction of the AVSat data from the ASat data yields a volume where only the veins are remaining but static tissue is suppressed. The principle of the c-GRAPPA method is depicted in Fig. 1. For the ASat data only the even k-space lines and for the AVSat data only the odd k-space lines are acquired (Fig. 1, step a). For corresponding slice positions central k-space lines from the ASat and the AVSat data are then combined to obtain calibration data for coil weight computation (Fig. 1, step b). These coil weights are used to reconstruct missing k-space lines for both, the ASat and the AVSat data. Fig. 2 depicts the principle of the z-GRAPPA method. The ASat data and the AVSat data are treated separately. For all slices of each data set the k-spaces are undersampled by a factor of R and for adjacent slices the acquired lines are shifted by one line (Fig. 2, step a). Calibration data is obtained by combining k-space lines from adjacent slices (Fig. 2, step b). The coil weights computed from that data are used to reconstruct the missing k-space lines (Fig. 2, step c). A fully sampled data set of the legs of one healthy volunteer was acquired using the described subtraction TOF venography method. Acquisition parameters were: TR/TE = 19.23/3.95ms, slices = 135, slice thickness = 3.5mm, FOV = 400x260mm², in plane resolution = 1.25x1.44mm². The following reconstructions were performed for both, the ASat and the AVSat data set: A conventional reconstruction from the fully sampled data, a conventional GRAPPA reconstruction, a z-GRAPPA and a c-GRAPPA reconstruction. For all GRAPPA reconstructions a reduction factor of $R = 2$ and 32 calibration lines were used. For conventional GRAPPA 16 extra calibration lines (which were also used for image reconstruction) were acquired for that purpose reducing the net acceleration of 1.71. The net acceleration for z-GRAPPA and c-GRAPPA was 2. The ASat and AVSat data sets reconstructed with the different methods were subtracted and images of the venous structure were obtained using a maximum intensity projection (MIP). Image quality was assessed by a region-of-interest analysis of the contrast-to-noise ratio between vein and muscle (CNR_{muscle}) for a proximal vein (v. femoralis) and a distal vein (v. tibialis posterior) in the axial slices marked in Fig. 3a.

Results

Figure 3 shows the MIPs resulting from the different reconstruction methods. For the GRAPPA based reconstructions only the right leg is displayed. Hardly any differences between the MIPs can be perceived. Figure 4 shows the CNR_{muscle} values for the different algorithms which are very similar for the fully sampled data and for the conventional GRAPPA reconstruction. The CNR_{muscle} values for z-GRAPPA and c-GRAPPA method are only slightly below. The artifact power computed over all slices for the different GRAPPA based reconstructions is displayed in Fig. 5. The lowest value is observed for conventional GRAPPA. The artifact power for the z-GRAPPA and the c-GRAPPA reconstruction is slightly higher with the artifact power for the c-GRAPPA reconstruction being highest.

Discussion

Two variants of the GRAPPA algorithm which do not require the acquisition of extra calibration data have successfully been applied to subtraction TOF venography with continuously moving table. Compared to the fully sampled measurements and to conventional GRAPPA only a minor loss in image quality was observed. The achieved speedup compared to conventional GRAPPA is 9%, i.e. the examination duration to image the legs as shown in Fig. 3 could potentially be reduced from 5:05min to 4:22min. The z-GRAPPA method requires small variations of the imaged anatomy and of the coil sensitivities in slice direction. Both requirements are optimally fulfilled for the studied data due to the small slice distance and the smooth variation of the peripheral veins in slice direction. The applicability of the c-GRAPPA method is limited by the differences between ASat and the AVSat data, which are besides the venous signal due to interscan motion artifacts. Future work includes the combination of c-GRAPPA with a different acquisition scheme for subtraction TOF venography [4] which minimizes to risk of motion artifacts between the acquisition of corresponding slices of the ASat and the AVSat data set. Furthermore, the diagnostic value of the z-GRAPPA and the c-GRAPPA method for TOF venography will have to be proven in clinical studies.

References

- [1] S. Huff et al.: Proc. of Int. Soc. Magn. Reson. Med., 2008; p. 926 [2] M. Griswold et al.: Magn Reson Med, 2002. 47(6): p. 1202-1210. [3] M. Honal et al.: Magn Reson Med, in press, 2008. [4] S. Huff et al.: Proc. of MR Angioclub, 2008.

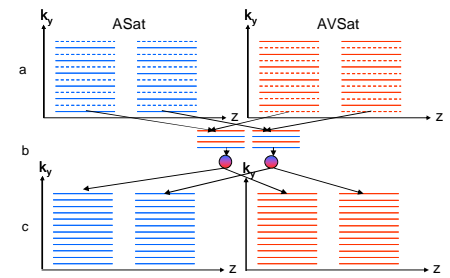


Fig. 1: Schematic description of c-GRAPPA.

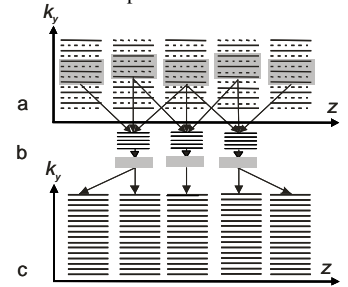


Fig. 2: Schematic description of z-GRAPPA.

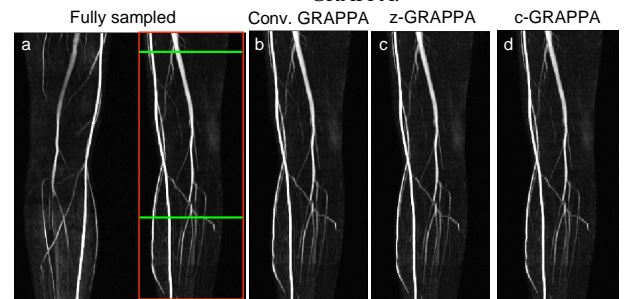


Fig. 3: MIPs of the different reconstructions. The slices used for CNR computation are indicated in the MIP of the fully sampled data.

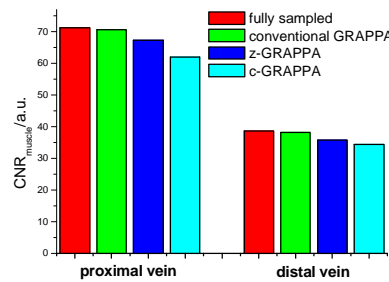


Fig. 4: CNR computed for two slices for the different reconstructions.

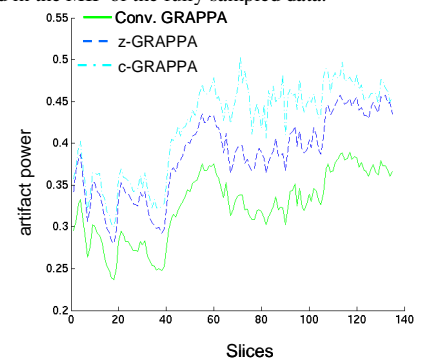


Fig. 5: Artifact power over all slices.